

CONTROL OF A MIXING LAYER FLOW BY FLUID INJECTION : DIRECT NUMERICAL SIMULATION RESULTS

Sylvain Lardeau

Laboratoire d'Etudes Aérodynamiques UMR 6609, Université de Poitiers,
Téléport 2 - Bd. Marie et Pierre Curie B.P. 30179, 86962 Futuroscope Chasseneuil Cedex, France
sylvain.lardeau@lea.univ-poitiers.fr

Eric Lamballais

eric.lamballais@lea.univ-poitiers.fr

Jean-Paul Bonnet

jean-paul.bonnet@lea.univ-poitiers.fr

ABSTRACT

In this paper, direct numerical simulations of a jet impacting a mixing layer are presented for purpose of flow control. Two points of view are considered : a control jet impacting Kelvin-Helmholtz eddies as well as its impact on a three-dimensional mixing layer. The control of the two-dimensional vortices with a steady control jet has permitted to built a simplified open-loop, based on the vertical velocity at the impact region, in order to actively control these vortices. Results of the control of a turbulent mixing layer show that the streamwise location of the impact is crucial.

INTRODUCTION

The control of turbulent free shear flows has numerous applications, especially in aerospace industries. Schematically, the goal of the control can be an increase of mixing properties of the flow (improvement of combustor efficiency) or a reduction of its acoustic emission (reactor noise). Among the various possibilities to perform the control action, the use of control jets on a free shear layer (see Delville et al.,2000 for a recent review) offers a major advantage: the action can be easily and rapidly adjusted by a simple modification of the control jets flow rate. Such a possibility is clearly attractive in the context of active control. This paper presents results from Direct Numerical Simulations (DNS) of the interaction between a small inclined jet and a spatially developing mixing layer. The goal of the present work is to consider various control configurations (modification of the pulsation or the velocity of the jet) in order to determine in each case

the consequences of the control on turbulent statistics and vortex dynamics. It is expected that a best knowledge of the links between statistical modification of the flow and its instantaneous structural feature (influence of/on coherent structures) can be helpful to define an optimal control strategy.

In the first part, the numerical methods and the flow parameters are presented. In the second part, the control of a mixing layer with Kelvin-Helmholtz (KH) vortices is considered for various control jet flow rates. The influence of the control jet on the spatial development of a turbulent mixing layer is studied in the third part of this work.

FLOW CONFIGURATION AND NUMERICAL METHODS

The interaction between an inclined jet and a mixing layer is considered in a Cartesian frame of reference $\mathcal{R} = (0; x, y, z)$. x, y and z are respectively the streamwise, transverse and spanwise directions (fig. 1). (u_x, u_y, u_z) are the velocity components. Free-slip condition is imposed in the transverse direction at $y = \pm L_y/2$. Periodic boundary condition is used in the spanwise direction, and the outflow condition is deduced by solving a simplified convective equation.

At the inflow section, a velocity profile of a round jet oriented by the angles φ and ψ (see figure 2 for angle definitions) is superimposed to velocities data corresponding to a plane mixing layer flow. By convention, the origin of the jet is placed on the Oy -axis at a distance d from the plane Oxz . We note x_m the streamwise location of the merging of the two flows, and u_c

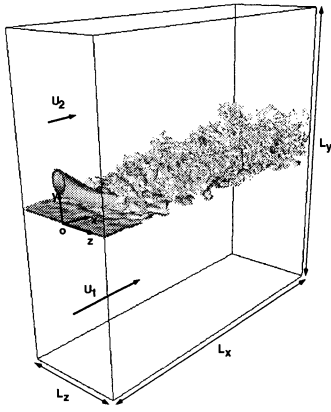


Figure 1: Computational domain and axis the jet centerline velocity.

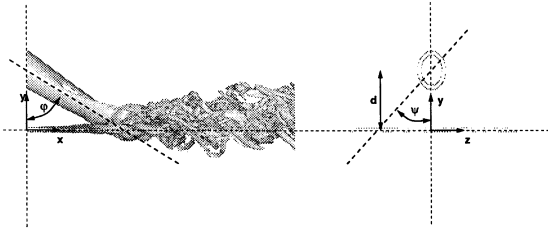


Figure 2: Angle definition

Indeed, the control effects are very different in terms of receptivity if the jet impacts in a transitional or in a fully turbulent region. That is why the choice of the impact region is crucial in control method. In order to adjust the region of impact, the inflow velocity field can be deduced from a precursor calculation. In this computation, the inflow mean velocity profile $\langle u_x \rangle (y)$ is given by an hyperbolic tangent with

$$\langle u_x \rangle (y) = \frac{U_1 + U_2}{2} - \frac{\Delta U}{2} \tanh\left(\frac{2y}{\delta_{\omega_i}}\right) \quad (1)$$

where δ_{ω_i} is the inflow vorticity thickness. U_1 and U_2 are respectively the high- and low-speed free-stream velocities, $\Delta U = U_1 - U_2$ is the velocity difference. Two types of velocity perturbations are used :

- to generate the mixing-layer roll-up at a given frequency, an harmonic perturbation is superimposed to the u_y -component of the velocity field. The Strouhal number, defined as $St = f_0 \delta_{\omega_i} / \Delta U$, is equal to $St = 0.066$.
- to generate a turbulent mixing layer, small random perturbations with a prescribed kinetic energy spectrum are superimposed to the three components of the velocity field in order to mimic residual turbulence.

During the precursor simulation, the velocity data at $x = 9\delta_{\omega_i}$ are saved at each time step.

Designation	(L_x, L_y, L_z)	(n_x, n_y, n_z)
ML2D***	$(122\delta_{\omega_i}, 86.4\delta_{\omega_i}, 43.2\delta_{\omega_i})$	$(245, 289, 144)$
ML3D***	$(122\delta_{\omega_i}, 115.2\delta_{\omega_i}, 43.2\delta_{\omega_i})$	$(245, 385, 144)$

Table 1: Flow configurations and simulation parameters

Designation	Radius of the control jet (R_c)	$u_{c_{max}}$	$u_{c_{min}}$
ML2DR	$0\delta_{\omega_i}$	$0\Delta U$	$0\Delta U$
ML2DSC	$1.5\delta_{\omega_i}$	$1\Delta U$	$1\Delta U$
ML2DUC1	$1.5\delta_{\omega_i}$	$0.5\Delta U$	$1.5\Delta U$
ML2DUC2	$1.5\delta_{\omega_i}$	$0.5\Delta U$	$1.5\Delta U$

Table 2: Flow parameters for the two-dimensional control case

Then, the stored data are used as inflow conditions during the jet/mixing-layer simulation.

The two parameters associated to the main flow are the Reynolds number $Re = \Delta U \delta_{\omega_i} / \nu$ and the velocity ratio $\lambda = \Delta U / (U_1 + U_2)$. The value of the Reynolds number is $Re = 200$. Two values of λ are considered : $\lambda = 0.66$ and $\lambda = 0.91$. The velocities associated to those values are respectively $(U_1, U_2) = (1.25\Delta U, 0.25\Delta U)$ and $(U_1, U_2) = (1.05\Delta U, 0.05\Delta U)$. These low velocities are imposed owing to the superposition of control jets. Hence, for higher velocity values, the control jet is too deviated. The incompressible Navier-Stokes equations are directly solved using a non-staggered grid with the number of grid points and mesh spacing shown in Table 1. Sixth-order compact centered difference schemes are used (Lele, 1992) to evaluate all spatial derivatives, except near the in- and out-flow boundaries where single sided schemes are employed for x -derivative calculation. Time integration is performed with a third-order Runge-Kutta method. To study control effects on mixing properties of the main flow, an additional passive scalar equation is solved. The initial profile of the scalar field T is similar to the longitudinal velocity profile (1), and vary from 0 in the low-speed stream to 1 in the high-speed stream.

CONTROL OF THE TWO-DIMENSIONAL STRUCTURES OF A MIXING LAYER

We consider first the control of an initially two-dimensional mixing layer by a control jet. The value of λ is 0.91. The u_z -component of the velocity field is set equal to zero at the inflow condition as well as the derivative in the z -direction. The inflow condition for the mixing layer is deduced from a precursor simulation of a two-dimensional mixing layer with the harmonic perturbation described above. In this simulation, the velocity field is saved at a distance $x_d = 9\delta_{\omega_i}$ from the inflow condition.

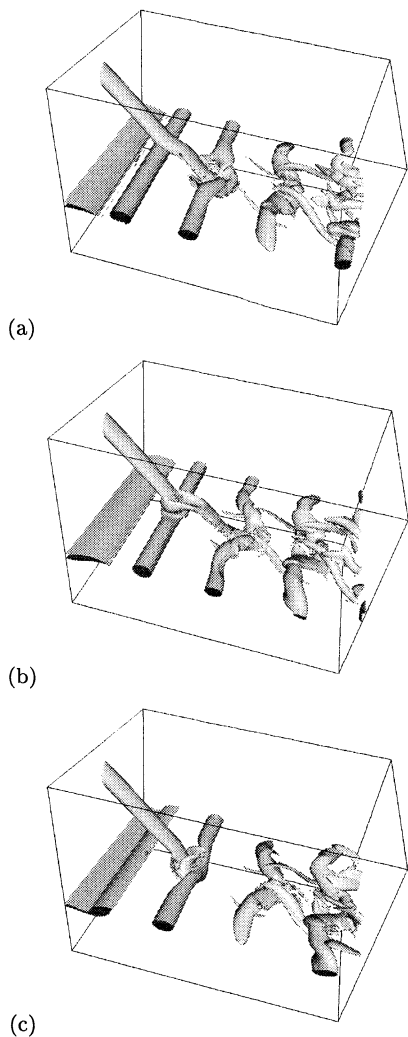


Figure 3: Isosurface of vorticity for $||\vec{\omega}|| = 0.5\Delta U/\delta\omega_i$ (case ML2DSC) (a) $t = 202.7\delta\omega_i/\Delta U$ (b) $t = 211.8\delta\omega_i/\Delta U$ (c) $t = 221.9\delta\omega_i/\Delta U$

Fig. 3 shows an isosurface of the vorticity modulus of a steady control jet impacting the mixing layer observed at three different instants corresponding to three positions of a KH vortex. It clearly appears that the penetration of the control jet in the mixing layer depends on the passage of the vortex. When the eddy is upstream x_m (fig. 3(a)), the control jet can't penetrate the shear layer and is deviated downstream. When the vortex crosses the impacted region (fig. 3(b)), the jet can enter the eddy. Then, the control jet winds around the bidimensional vortex (fig. 3(c)).

The velocity field (fig. 4) shows the flapping of the control jet in the $(0, x, y)$ plane. This kind of unstable mode has been observed by Delville et al. (2000). It can be inferred that this flapping is due to coherent structures passing through the shear layer. In order to simplify the flow description, we can decompose the vortex in four parts (points), in

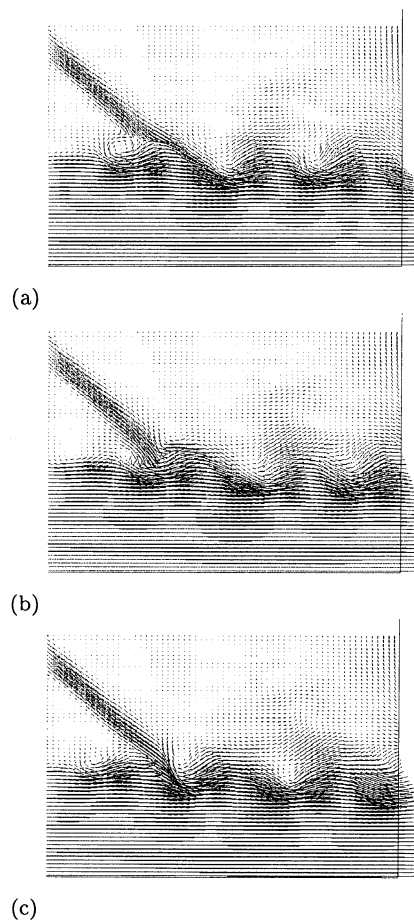


Figure 4: Velocity field for the simulation ML2DSC (a) $t = 202.7\delta\omega_i/\Delta U$ (b) $t = 211.8\delta\omega_i/\Delta U$ (c) $t = 221.9\delta\omega_i/\Delta U$

accordance with its vertical velocity (fig. 5). Then, we can assume that the flapping is due to the variation of the local vertical velocity. Upstream of the KH eddy (point A and B), the vertical velocity is negative and the jet can penetrate the shear layer, creating an acceleration of the rotation. When the jet impacts downstream of the vortex (point C and D, fig. 4), the induced velocity creates with the peripheral velocity of the KH eddy a shear which can give rise to an absolute instability process.

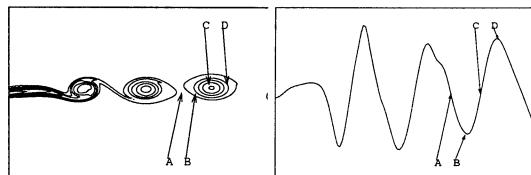


Figure 5: Vorticity isocontour (left) and vertical velocity on the axis (right) for the 2D simulation

This analysis is used to built an open-loop for an active control of KH eddies. For the next two simulations, the control jet flow rate is driven by the time variation of the vertical velocity at $x = x_m$. The difference between those simulations is the phase of the pulsation.

The first phase was chosen so that the jet impact the flow on KH vortices (corresponding to point *C*, fig. 4). In this case, the control jet velocity and vertical velocity at $x = x_m$ are shown on fig. 6. These profiles are obtained from two separate simulations, one of the non-controlled mixing layer, and the other of an inclined jet alone. Figs. 7, 8 and 9 show

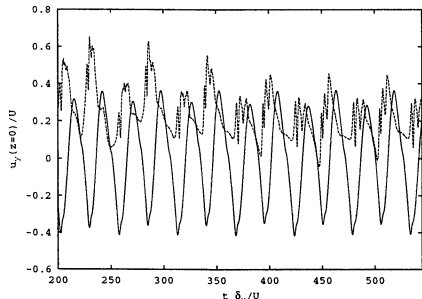


Figure 6: Comparison of the vertical velocity (u_y) of the natural mixing layer (—) and the velocity of the control jet (---)

an isosurface of vorticity modulus for the two simulations at different instants. The choice of the phase of the jet velocity has clearly an influence on the spatial development of the mixing layer. For the simulation ML2DUC1, the jet penetrates the vortex (fig. 8). When the phase is chosen so that the jet impacts upstream of the eddy (point *B*, fig. 5), the penetration is maximum and small scale transition seems to be more effective. We can compare the control impact by comparing the maximum of the vorticity modulus. Hence, this maximum is observed for the case ML2DUC2 (impact upstream of the vortex), with $\|\vec{\omega}\| = 3\Delta U/\delta_{\omega_i}$. For the two other simulations, the maximum are $\|\vec{\omega}\| = 1.8\Delta U/\delta_{\omega_i}$ and $\|\vec{\omega}\| = 2.4\Delta U/\delta_{\omega_i}$ respectively for the simulations ML2DSC and ML2DUC1. This behavior can be related to the acceleration of the rotation in the case ML2DUC2. The vortex dynamic is very complex, and the results of the active control show that the choice of the time of the impact (or the region of the eddy) is crucial.

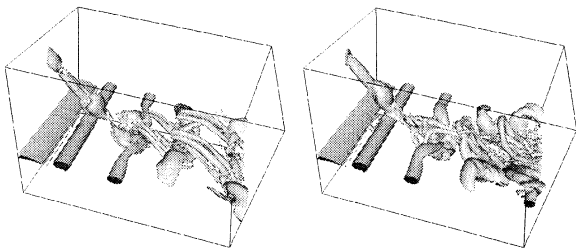


Figure 7: Isosurface of vorticity for $\|\vec{\omega}\| = 0.5\Delta U/\delta_{\omega_i}$ at $t = 201.7\delta_{\omega_i}/\Delta U$ (a) ML2DUC1 (b) ML2DUC2

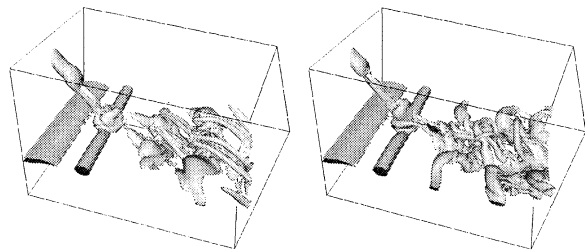


Figure 8: Isosurface of vorticity for $\|\vec{\omega}\| = 0.5\Delta U/\delta_{\omega_i}$ at $t = 211.8\delta_{\omega_i}/\Delta U$ (a) ML2DUC1 (b) ML2DUC2

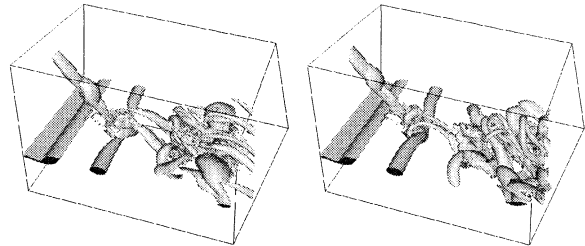


Figure 9: Isosurface of vorticity for $\|\vec{\omega}\| = 0.5\Delta U/\delta_{\omega_i}$ at $t = 221.9\delta_{\omega_i}/\Delta U$ (a) ML2DUC1 (b) ML2DUC2

Designation	λ	Mean control jet flow rate	u_c
ML3DR1	0.91	0	0
ML3DR2	0.66	0	0
ML3DSC1	0.91	1	1
ML3DSC2	0.91	1.5	1
ML3DSC3	0.66	1.5	1

Table 3: Flow parameters for five three-dimensional cases

CONTROL OF A TURBULENT MIXING LAYER

The control of a fully turbulent mixing layer is presented here. The first part of this section deals with the qualification of the simulation of mixing layer for high values of λ . In the second part, the control of those shear layer are presented. For the control cases, two parameters are modified : the jet centerline velocity u_c and the region of impact. Flow parameters for each case are shown in table 3.

Validation of the natural mixing layer

Fig. 10 and 11 show an isosurface of the vorticity modulus of the natural mixing layers. Common features of spatial mixing layer transition are recovered. We observe the high degree of the three-dimensionality of the flow due to the isotropic nature of the inflow perturbations in agreement with previous works (Comte et al., 1992, Comte et al., 1998).

The statistics are computed at $x/\delta_{\omega_i} = 137$ and $x/\delta_{\omega_i} = 80$ for respectively $\lambda = 0.66$ and $\lambda = 0.91$. Note that those positions are *a priori* larger than the corresponding stream-wise distance where self-similar regime has been observed. For example, Bell and Metha

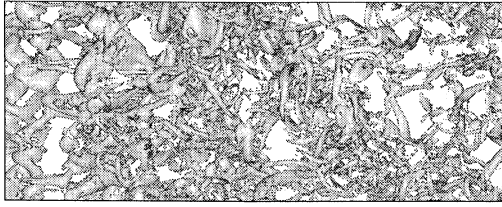


Figure 10: Isosurface of vorticity for $\|\vec{\omega}\| = 0.5\Delta U/\delta_{\omega_i}$ in the $(0; x; y)$ plane for the simulation ML3DR1

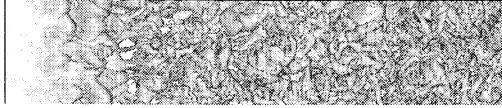


Figure 11: Isosurface of vorticity for $\|\vec{\omega}\| = 0.5\Delta U/\delta_{\omega_i}$ in the $(0; x; y)$ plane for the simulation ML3DR2

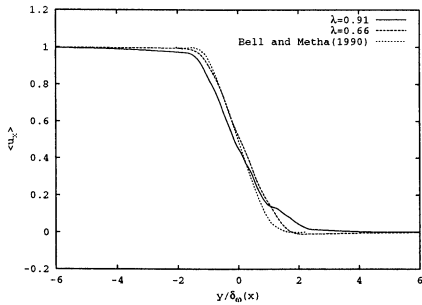


Figure 12: Mean velocity profiles for the cases ML3DR1 and ML3DR2 compared to the result of Bell and Metha(1990)

(1990) have estimated that for $\lambda = 0.25$, self-similar conditions start from $x \approx 250\delta_{\omega_i}$. For the present simulations, such a position corresponds to $x \approx 95\delta_{\omega_i}$ for $\lambda = 0.66$ and $x \approx 70\delta_{\omega_i}$ for $\lambda = 0.91$. However, it can be noticed that at the end of the computational domain, the shear layer is too close to the free-slip condition. Hence, only a part of the computational domain can be used for statistical computations. Comparisons of the statistics show a quite good agreement, in spite of a lack of convergence and a difference of Reynolds number.

The mean velocity profiles corresponding to the two simulations are plotted with self-similar scaling on fig. 12. Also included are the experimental data of Bell and Metha (1990) for a turbulent mixing layer. The Reynolds stress profiles $\langle u_i u_i \rangle$ are also compared to there experimental results (fig. 13). The numerical profiles have been shifted to center them at $y = 0$, thus accounting for the drift of the center of the layer into the low-speed stream.

Control of the turbulent mixing layer

The first case considered is the control of the mixing layer for $\lambda = 0.91$. Two values of the control jet velocity are used : $u_c = 1\Delta U$ and $u_c = 1.5\Delta U$. For those simulations, inflow

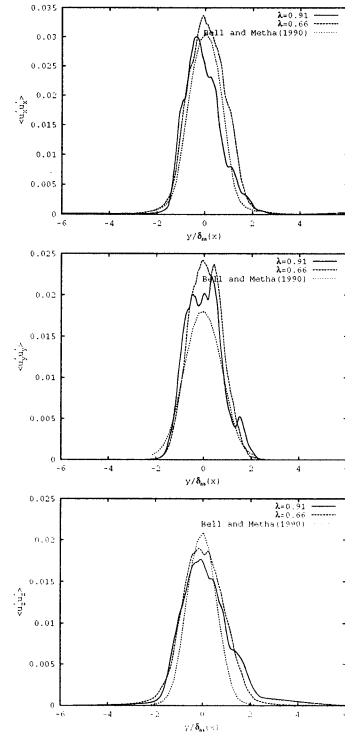


Figure 13: Comparison of the natural mixing layer results for the components of the Reynolds stress tensor with the results of Bell and Metha(1990)

data are deduced from a precursor simulation in order to impact in a turbulent region. Instantaneous visualizations for the two cases are shown on figs. 14 and 15. No major effects on three-dimensional structures can be observed. However, small-scale transition seems to be more active for *ML3DSC2*.

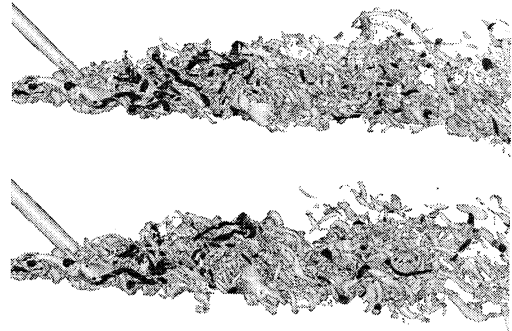


Figure 14: Isosurface of vorticity $\|\vec{\omega}\| = 0.5\Delta U/\delta_{\omega_i}$ in the $(0; x; y)$ plane for (top) ML3DSC1 (bottom) ML3DSC2

The second case considered is the mixing layer for $\lambda = 0.66$, shown on fig. 16. The impact region chosen in this case corresponds to the transition region. The organization of coherent structures is strongly affected by the injection of the fluid in the shear layer. In the neighborhood of the impact region, well organized structures can be observed on the contrary to the case without control jet where at the same downstream position (see fig. 11),

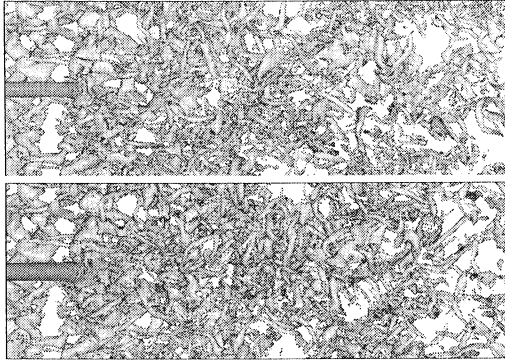


Figure 15: Isosurface of vorticity $||\vec{\omega}|| = 0.5\Delta U/\delta\omega_i$ in the $(0; x; z)$ plane (top) ML3DSC1 (bottom) ML3DSC2

small scales seem to be more active. Nevertheless, in the peripheral region of the impact, small scale transition seems to be more effective in the controlled case. A possible scenario

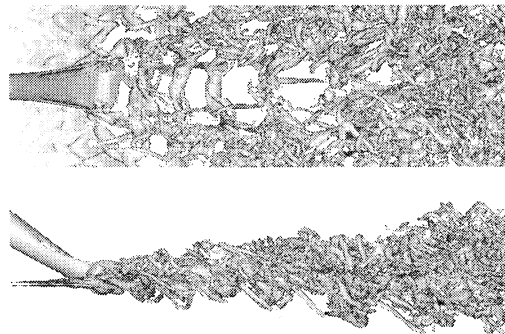


Figure 16: Isosurface vorticity for $||\vec{\omega}|| = 0.5\Delta U/\delta\omega_i$ in the $(0; x; y)$ plane for (top) ML3DSC1 (bottom) ML3DSC2

is that the control jet, which is strongly deviated by the low-speed stream, creates a strong vertical gradient on a significant spanwise extent. Then, this gradient allows for an inflexional instability, that can lead to KH type local instability. This effect can be used to built new control strategies. It can be noticed that for the three cases, the injection of the streamwise vorticity in the mean flow is not significant, as observed for the control of round jets (Lardeau et al., 2001).

Comparisons of the probability density function (PDF) of the scalar field are shown on fig. 17. Two cases are considered : the region near the impact (fig. 17(a)) and the self-similar region (fig .17(b)). No data of the passive scalar are available for the case *ML3DSC3*. As mentioned above, the effect of control jet is not significant, PDF evolution is quasi-similar for the three cases.

CONCLUSION

The vortex dynamic of the interaction mixing layer/control jet has been studied. First,

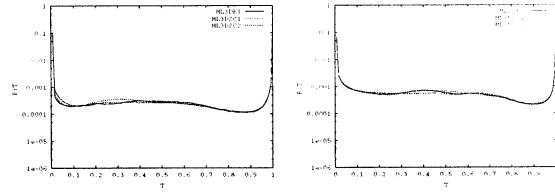


Figure 17: Comparison of the PDF of the scalar field for the three simulations for $\lambda = 0.91$ at (top) $x/\delta\omega_i = 40$ (bottom) $x/\delta\omega_i = 80$

the impact of a control jet on KH eddies has shown that the time of the impact (corresponding to a region of an eddy) is crucial. The modification of this region give rise to different type of instabilities (absolute or rotationnal). A possible scenario based on the interaction of the jet momentum and the incoming eddy characteristics finds to define some active control method. In the turbulent mixing layer, the absence of bidimensional structures make the control action less efficient. However, for appropriate velocity ratio, the control-jet is deviated enough in such a way that quasi-2D structures are created.

ACKNOWLEDGMENT

Computations were carried out at the Institut du Développement et des Ressources en Informatique Scientifique, CNRS, Paris.

REFERENCES

- Bell, J., and Metha, R., 1990, "Development of a two-stream mixing layer from tripped and untripped boundary layers", *AIAA Journal*, Vol. 28, pp 2034-2042.
- Comte, P., Lesieur, M., and Lamballais, E., 1992, "Large- and small-scale stirring of vorticity and a passive scalar in a 3-d temporal mixing layer", *Phys. Fluids A*, Vol. 4(12), pp 2761-2778.
- Comte, P., Silvestrini, J.H., Bégou, P., 1998, "Streamwise vortices in large-eddy simulations of mixing layers", *Eur. J. Mech. B/Fluids*, Vol. 17(4), pp 615-637.
- Delville, J., Collin, E., Lardeau, S., Lamballais, E., Barre S., and J.P. Bonnet., 2000, "Control of jets by radial fluid injection", *ERCOFTAC Bulletin*, Vol. 44, pp 57-67.
- Lardeau, S., Lamballais, E., and Bonnet, J.P., 2001, "Direct numerical simulation of a controlled jet by fluid injection", *J. Turb.*, in preparation.
- Lele, S.K., 1992, "Compact Finite difference schemes with spectral like resolution", *J. Comp. Phys.*, Vol. 103, pp 16-42.